

# Effects of Intensity Thresholding on the Power Spectrum of Laser Speckle

Alfred D. Ducharme and Glenn D. Boreman

University of Central Florida  
Center for Research in Electro-Optics and Lasers  
Orlando, FL 32816

Donald R. Snyder

Wright Laboratory WL/MNGI  
Eglin A.F.B., FL 32542

## ABSTRACT

Spatial-frequency filtering of laser speckle patterns has proven to be a useful tool in the measurement of MTF for focal plane arrays. Intensity thresholding of the laser speckle patterns offers nearly an order of magnitude savings in digital storage space. The effect of this thresholding on the spatial-frequency power spectral density of the speckle pattern is investigated. An optimum threshold level is found that minimizes distortion of the power spectrum for the classes of speckle data used for MTF testing.

## 1. INTRODUCTION

The statistics of speckle phenomena have been the focus of many research efforts since the introduction of the laser. As our knowledge of speckle behavior increases, new ways to use and control it become evident. One useful application of laser speckle has been the measurement of modulation transfer function (MTF) of CCD arrays.<sup>1</sup> In this application a considerable amount of laser speckle data is collected for each MTF calculation which must be stored digitally for future use. Because digital storage space is always a problem, it is desirable to reduce the amount space required by this application.

The size of the data arrays used in the calculation are fixed by the size of the CCD array being tested, meaning only two ways to reduce the data exist. First, the number of points used to plot the MTF could be minimized. This would reduce the accuracy of the calculation because the spacing of data points dictates the size fluctuation in MTF that can be detected. Second, the speckle intensity could be thresholded eliminating all but 2 of the 256 gray levels used to represent the digitized speckle field (Fig. 1). This binarization would transform the 8-bit data into 1-bit data, reducing the total amount of data by nearly an order of magnitude.

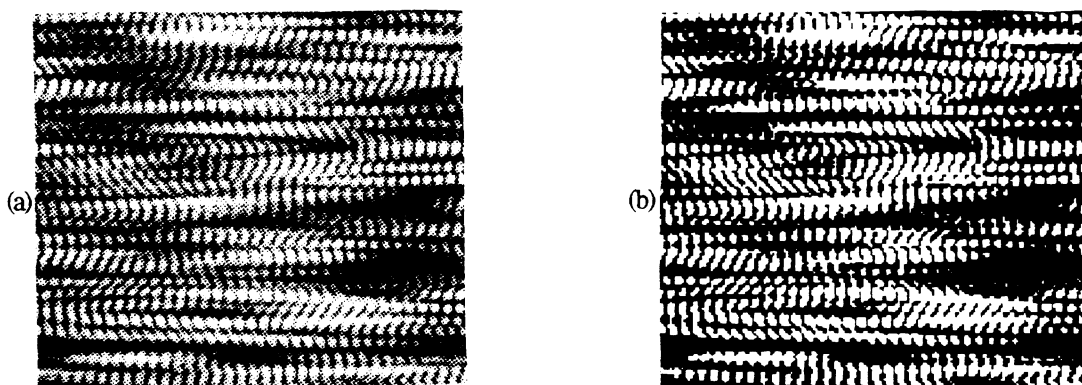


Fig. 1. Narrowband laser speckle: (a) Continuous laser speckle with 256 gray levels.  
(b) Laser speckle reduced to 2 gray levels by thresholding at the mean intensity.

This paper shows that the fidelity of the spatial-frequency power spectral density of the laser speckle intensity is maintained after a thresholding operation is performed. The effects of the intensity thresholding will be investigated and an optimal threshold value will be determined for the narrowband laser speckle used in the MTF calculation.

The second section of this paper discusses the derivation of the spatial autocorrelation function for the continuous and thresholded intensity of the laser speckle. The derivation will be exemplified using two different cases. The first case will be a simple square aperture and the second will be a double-slit aperture used in the calculation of MTF.

The relationship between the autocorrelation and power spectral density of the thresholded laser speckle will be discussed in the third section. The same two examples will be used, and an optimal threshold level will be determined for each case based on a minimum-mean-squared-error analysis in their power spectral densities. A computer simulation of these two examples was performed to check the validity of this analysis and its results are given in section 4 in terms of power spectrum.

## 2. AUTOCORRELATION OF THRESHOLDED LASER SPECKLE

In this section we will derive the spatial autocorrelation function for intensity thresholded laser speckle. To simplify the reading, this function will be referred to as the *thresholded autocorrelation*. The derivation will begin with the spatial autocorrelation function for intensity distribution of nonthresholded laser speckle, which will be referred to as the *continuous autocorrelation*.

The continuous autocorrelation is measured using two observations of the speckle intensity. Ideally, these observations are made using two point detectors that sample the speckle field simultaneously at different points in a common plane  $(x,y)$ . The autocorrelation is formed by finding the expected value of the product of the two observations for each unique separation distance. This is expressed as,<sup>2</sup>

$$R_I(x_1, y_1; x_2, y_2) = \langle I(x_1, y_1) I(x_2, y_2) \rangle. \quad (1)$$

In reality the detectors are of finite size, which changes the overall shape of the autocorrelation by convolving Eq. (1) by the spatial autocorrelation of a single detector. This paper omits the added effect of finite detector size so that the singular effect of thresholding could be investigated.

The only factor contributing to the form of the spatial autocorrelation is the amplitude of the field emanating from the generating aperture,  $P(\xi, \eta)$ . This relationship is described by Goodman<sup>2</sup> as

$$R_I(\Delta x, \Delta y) = \langle I \rangle^2 \left[ 1 + \frac{\left| \iint_{-\infty}^{\infty} |P(\xi, \eta)|^2 \exp\left[i \frac{2\pi}{\lambda z} (\xi \Delta x + \eta \Delta y)\right] d\xi d\eta \right|^2}{\iint_{-\infty}^{\infty} |P(\xi, \eta)|^2 d\xi d\eta} \right]. \quad (2)$$

From this we can see that the continuous autocorrelation is basically the magnitude squared of the Fourier transform of  $P(\xi, \eta)$ . As a result, using Eq. (2) we can calculate an analytical expression for the continuous autocorrelation for any generating aperture which exists physically.

Our goal is to determine the thresholded autocorrelation,  $R_I^{(b)}$ . We must determine a relationship between the continuous and thresholded autocorrelations. The speckle field is thresholded using the following operator,

$$I^{(b)}(x, y) = \begin{cases} 1, & \text{if } I(x, y) \geq b \langle I(x, y) \rangle \\ 0, & \text{if } I(x, y) < b \langle I(x, y) \rangle \end{cases}. \quad (3)$$

The thresholded autocorrelation can be determined from the continuous autocorrelation using a relationship calculated by

Barakat,<sup>3</sup>

$$R_I^{(b)}(\Delta x, \Delta y) = \frac{\Gamma^2(\alpha, b\alpha)}{\Gamma^2(\alpha)} + \frac{(b\alpha)^{2\alpha} \exp(-2b\alpha)}{\Gamma^2(\alpha)} \sum_{n=1}^{\infty} \frac{(R_I(\Delta x, \Delta y))^n}{\binom{n+\alpha-1}{n}} (L_{n-1}^{(\alpha)}(b\alpha))^2, \quad (4)$$

where  $\Gamma$  is the complimentary incomplete gamma function and  $L_{n-1}^{(\alpha)}$  is the associated Laguerre polynomial.<sup>5</sup> The parameter  $\alpha$  is equivalent to the mean of the intensity squared divided by the variance. In this paper we are assuming point detectors meaning that the value of  $\alpha$  is equal to 1. Using  $\alpha=1$ , Eq. (4) can be simplified to

$$R_I^{(b)}(\Delta x, \Delta y) = \exp(-b) \left[ 1 + b^2 \sum_{n=1}^{\infty} \frac{(R_I(\Delta x, \Delta y))^n}{n^2} (L_{n-1}^{(1)}(b))^2 \right]. \quad (5)$$

This equation was computed utilizing the recursion formula for Laguerre polynomials<sup>5</sup> over the range of possible correlation values (0.0 to 1.0). The result is given in Fig. 2 in the form of a mapping. A value of continuous autocorrelation,  $R_I$ , can be mapped to the corresponding value of thresholded autocorrelation,  $R_I^{(b)}$ , using Fig. 2. As an example, for a threshold value of  $b = 3$  a value of continuous autocorrelation,  $R_I = 0.4$ , would map to a value of thresholded autocorrelation,  $R_I^{(3)} = 0.25$ . Repeating this procedure for all values on a continuous autocorrelation function would yield the thresholded autocorrelation for a particular threshold value.

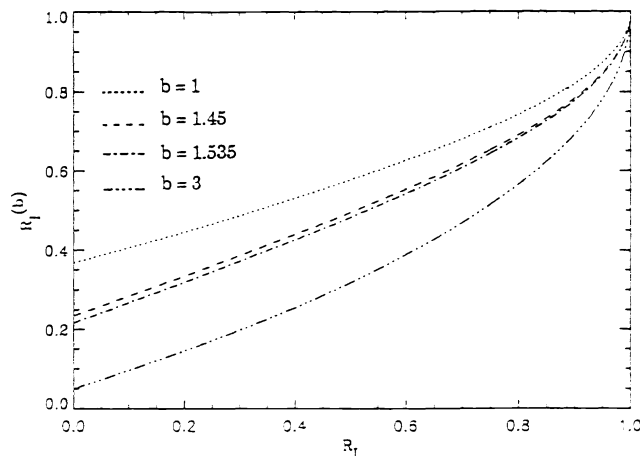


Fig. 2. Mapping for continuous autocorrelation,  $R_I$ , to thresholded autocorrelation,  $R_I^{(b)}$ , for threshold levels:  $b = 1, 1.45, 1.535,$  and  $3$ .

Two cases will be used to exemplify this mapping technique. One, a simple square aperture whose continuous autocorrelation can be found in Goodman.<sup>3</sup> Two, a double-slit aperture that was used in Ref. 1 to produce narrowband filtered laser speckle (Fig. 1).

The amplitude of the field emanating from a square aperture is expressed as

$$|P(\xi, \eta)|^2 = \text{rect} \frac{\xi}{L} \text{rect} \frac{\eta}{L}, \quad (6)$$

where  $L$  is the measure of each side of the square aperture. Substituting Eq. (6) into eq. (2) we find the continuous autocorrelation to be

$$R_I(\Delta x, \Delta y) = \langle I \rangle^2 \left[ 1 + \text{sinc}^2 \frac{L \Delta x}{\lambda z} \text{sinc}^2 \frac{L \Delta y}{\lambda z} \right]. \quad (7)$$

This is illustrated in Fig. 3 (solid line) for a single dimension with the bias level,  $\langle I \rangle^2$ , subtracted out. The autocorrelation was normalized so the correlation values would range from 0.0 to 1.0. Each value on the solid line in Fig. 3 is transformed by finding the corresponding value in Fig. 2. This was done to form the three new curves (dotted lines) which represent the thresholded autocorrelations for different threshold values.

For the second case the amplitude of the field emanating from the double-slit aperture is expressed as

$$|P(\xi, \eta)|^2 = \text{rect} \frac{\xi}{l_1} \text{rect} \frac{\eta}{l_2} * \left[ \frac{2}{L} \delta \delta \left( \frac{2}{L} \xi \right) \right], \quad (8)$$

where  $l_1$  and  $l_2$  are the width and height, respectively, of each rectangle and  $L$  is their separation distance in  $x$ . The continuous autocorrelation is given by Eq. (2);

$$R_I(\Delta x, \Delta y) = \langle I \rangle^2 \left[ 1 + \text{sinc}^2 \left( \frac{l_1 \Delta x}{\lambda z} \right) \text{sinc}^2 \left( \frac{l_2 \Delta y}{\lambda z} \right) \cos^2(\pi L \Delta x) \right]. \quad (9)$$

Once again, the thresholded autocorrelation can be determined using Eq. (9) and the correlation mappings in Fig. 2. The resulting thresholded autocorrelations for three different threshold values are shown in Fig. 4. Only the ' $\Delta x$ ' axis is plotted because the cosine term in Eq. (9) is in ' $\Delta x$ '.

The predominant change seen in the transformation of continuous-to-thresholded autocorrelation is the addition of a correlation bias, which results from a reduction in the uniqueness of the individual speckles. Consider the speckle intensity on a single dimension. The continuous speckles differ from each other in maximum intensity, length, and the rate that the intensity rises to and falls from the maximum intensity. Because each speckle is unique, the correlation tends to zero for large separation distances. The thresholded speckle intensity appears like a 'boxcar' signal with each speckle represented by a single box. The speckles all have the same intensity value and only differ in length. Since, each box 'looks' like every other box except for scaling, there will always be some bias correlation. This effect can be seen in Figs. 3 and 4. The amount of bias is equal to  $\exp(-b)$  which can be determined by evaluating Eq. (5) for  $R_I(\Delta x, \Delta y) = 0$

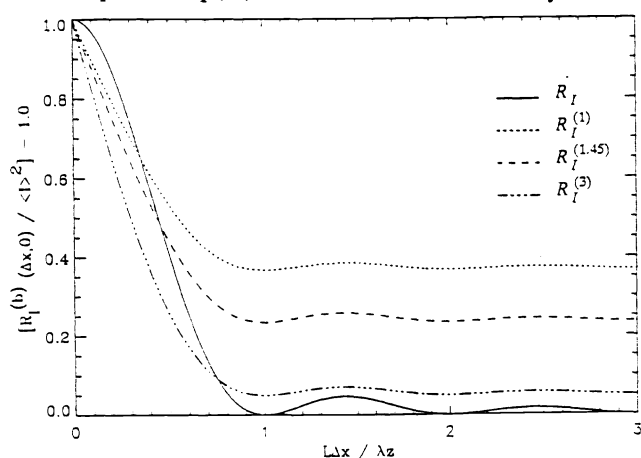


Fig. 3. Autocorrelation function of the speckle intensity resulting from a square aperture.

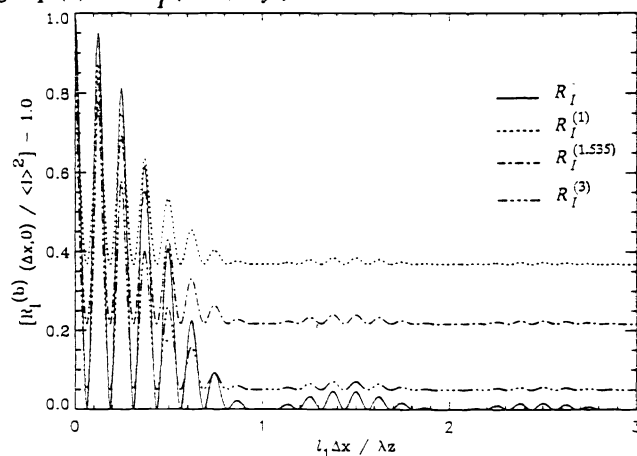


Fig. 4. Autocorrelation function of the laser speckle intensity resulting from a double-slit aperture.

### 3. POWER SPECTRUM OF THRESHOLDED LASER SPECKLE

The power spectral density is the frequency domain counterpart of the autocorrelation function. This relationship is described by the Wiener-Kinchine theorem<sup>4</sup> and is expressed as

$$S_I(v_x, v_y) = \mathcal{F}\{R_I(\Delta x, \Delta y)\}. \quad (10)$$

The power spectral density describes the amount of power that exists at each spatial frequency in the laser-speckle intensity distribution. Thresholding the speckle intensity may distort this distribution considerably if the correct threshold level is not chosen. An optimal threshold level occurs when the mean-squared error between the continuous and thresholded power spectrum is minimized. Where the continuous and thresholded power spectrums follow the terminology convention defined in the second section.

The continuous power spectrum for the square scattering area can be calculated by Fourier transforming Eq. (7) which yields

$$S_I(v_x, v_y) = \langle I \rangle^2 \left[ \delta(v_x, v_y) + \left( \frac{\lambda z}{L} \right)^2 \Lambda\left( \frac{\lambda z}{L} v_x \right) \Lambda\left( \frac{\lambda z}{L} v_y \right) \right]. \quad (11)$$

This expression is the reference from which the mean-squared error will be determined. The reference curve is shown as a solid line in Fig. 5. To find the thresholded power spectrum the thresholded autocorrelation is Fourier transformed numerically. This was done for three different threshold values (Fig. 5, dotted lines). The impulse function at the origin in Fig. 5 comes from the correlation bias described at the end of the section 2.

An analysis of Fig. 5 shows that the thresholded curves approach the shape of the continuous reference curve as the threshold level is increased from  $b=1.0$  to  $b=1.45$ . As the threshold level is increased further, the thresholded curve moves away from the reference. To determine it exactly, the mean-squared error in the power spectral density from  $nx = 0$  to  $nx = 200L/lz$  was calculated for threshold values between  $b=1.0$  and  $b=3.0$  (Fig. 6). A value of  $b=1.45$  was determined as the absolute minima and subsequent optimal threshold for the square aperture.

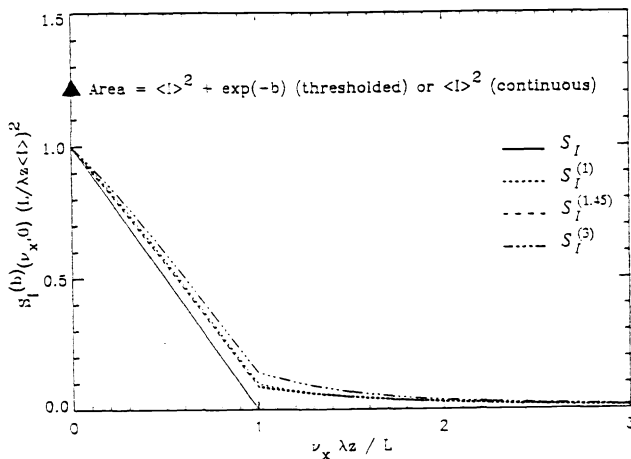


Fig. 5 Power spectral density of the laser speckle intensity resulting from a square aperture. Area refers to the strength of the impulse function.

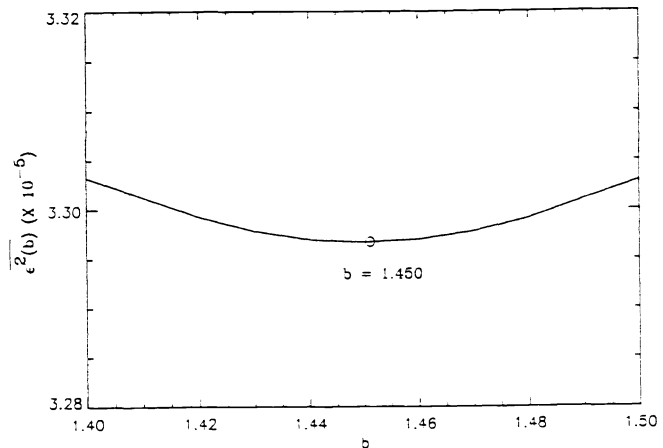


Fig. 6. Mean-squared error found in power spectral density of square aperture as a function of threshold value,  $b$ .

The same technique was applied to the double-slit aperture. From Eq. (9) the reference power spectrum is

$$S_I(v_x, v_y) = \langle I \rangle^2 \left\{ \delta(v_x, v_y) + \frac{1}{2} \frac{(\lambda z)^2}{l_1 l_2} \Lambda\left[\frac{\lambda z}{l_1} v_x\right] \Lambda\left[\frac{\lambda z}{l_2} v_y\right] + \frac{1}{4} \frac{(\lambda z)^2}{l_1 l_2} \Lambda\left[\frac{\lambda z}{l_1} \left(v_x - \frac{L}{\lambda z}\right)\right] \Lambda\left[\frac{\lambda z}{l_2} v_y\right] + \frac{1}{4} \frac{(\lambda z)^2}{l_1 l_2} \Lambda\left[\frac{\lambda z}{l_1} \left(v_x + \frac{L}{\lambda z}\right)\right] \Lambda\left[\frac{\lambda z}{l_2} v_y\right] \right\}. \quad (12)$$

The thresholded power spectrums for three threshold values are given in Fig. 7. Although the lines are closely spaced, further inspection shows that the thresholded power spectrum exhibits the same behavior seen in the first case. The mean-squared error calculation in the power spectral density was calculated from  $\nu_x = L/2lz$  to  $\nu_x = 3L/2lz$ . This limited range was used so that the optimal threshold value would be associated with the least amount of distortion in the outer triangle. The result was an optimal threshold value of  $b=1.535$  (Fig. 8).

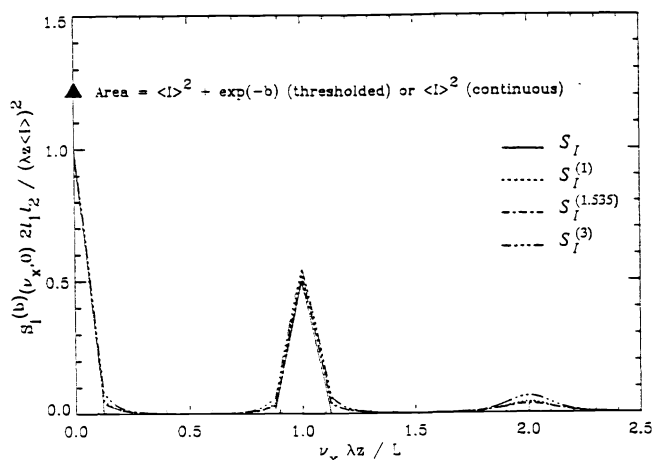


Fig. 7. Power spectral density of the laser speckle intensity resulting from a double-slit aperture. Area refers to the strength of the impulse function.

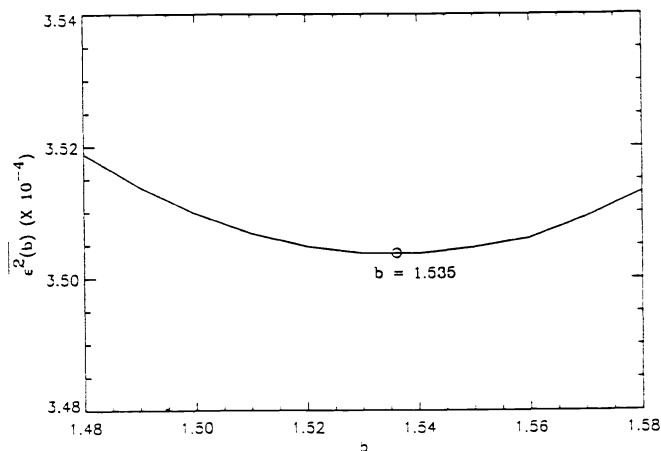


Fig. 8. Mean-squared error found in power spectral density of double-slit aperture as a function of threshold value,  $b$ .

#### 4. THRESHOLDED LASER SPECKLE SIMULATION

To verify the shape of the power spectral density for the optimal threshold values obtained in section 3, a Monte-Carlo simulation was performed. The simulation began by numerically propagating light, with unit magnitude and uniformly distributed  $(-\pi, \pi)$  phase, from each generating aperture. This created a large continuous one-dimensional data record containing simulated laser speckle. The record was then separated into several segments of equal length. The power spectrum was calculated for each segment and averaged together to form an estimate of the continuous power spectrum for the entire record.

To calculate estimates for the thresholded power spectrums the original data record was first thresholded at the optimal threshold value. The resulting binarized record was segmented and the estimates were calculated as before.

The results of the simulation are given in Figs. 9 and 10. The raw data was plotted as single points in both figures. The solid lines are the results determined in Section 3 for the optimal threshold values. The data show an increase of deviation with a decrease in frequency. This effect was expected, because the record is of finite length and there are less low frequency

speckles with which to form an average. A decrease in deviation is often seen in simulations of this type as the number of segments averaged is increased.

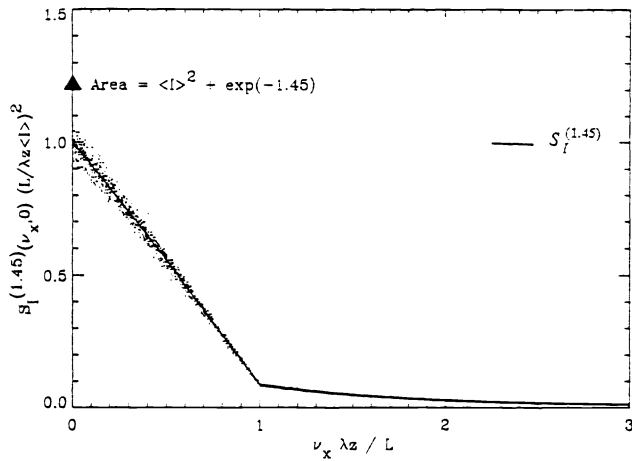


Fig. 9. Power spectral density of simulated laser speckle generated with square aperture and thresholded at  $b = 1.45$ . Area refers to the strength of the impulse function.

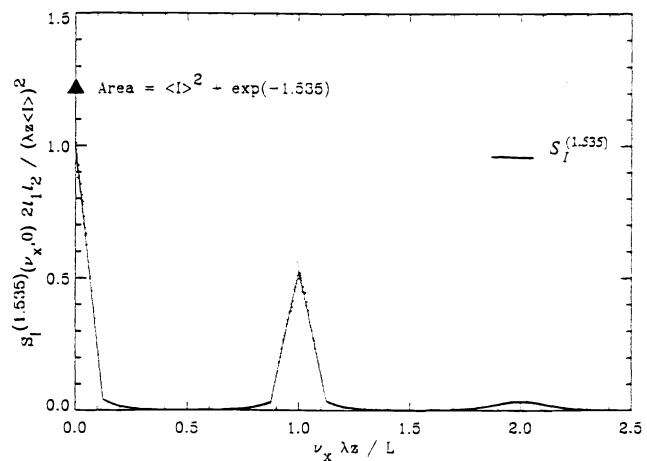


Fig. 10. Power spectral density of simulated laser speckle generated with double-slit aperture and thresholded at  $b = 1.535$ . Area refers to strength of impulse function.

## 5. CONCLUSIONS

The results presented here show that thresholding performed at the optimal level is a viable method for data reduction. We have shown that, for the MTF application, the important information is contained in the placement and size of the speckles and not in the intensity fluctuation between them. The thresholding operation preserves the important information and discards the rest, which is the methodology behind all data-reduction techniques. Implementation of this technique would result in an 8-to-1 savings in digital storage space.

## 6. ACKNOWLEDGMENTS

This work was supported by the U.S. Air Force office of Scientific Research under contract F49620-90-C-0076.

## 7. REFERENCES

1. M. Sensiper, G. Boreman, A. Ducharme, D. Snyder, "Modulation transfer function testing of detector arrays using narrow-band laser speckle," *Optical Engineering*, Vol. 32 No. 2, pp. 395-400, Feb. 1993.
2. R. Barakat, "Clipped Correlation functions of Aperture Integrated Laser Speckle," *Appl. Opt.* 25, p. 3885, 1986.
3. J. Goodman, *Laser Speckle and Related Phenomena*, J.C. Dainty, ed., pp. 35-40, Springer-Verlag, Berlin, 1975.
4. G.R. Cooper, C.D. McGillem, *Probabilistic Methods of Signal and System Analysis*, p. 253, 2nd ed., Holt, Rinehart and Winston, Inc., New York, 1971.
5. L.C. Andrews, *Special Functions for Engineers and Applied Mathematicians*, p. 179, Macmillan Pub. Co., New York, 1985.